https://doi.org/10.5194/egusphere-2026-3901
Preprint. Discussion started: 28 July 2026


# Technical note: From coccolith counts to quantitative carbonate fluxes: three decades of AI-assisted automated coccolith analysis

Luc Beaufort [1], Denis Dollfus[1,2], Yves Gally[1], Nicolas Barbarin[1], Martin Tetard[1,3], Baptiste Sucheras-Marx[1], Alexander Nistor[1], Mathieu Biaut[1]

[1]Aix-Marseille Univ., CNRS, IRD, INRAE, CEREGE, 13090, Aix-en-Provence, France

[2] London Stock Exchange Group, 75002 Paris, France

[3] ESNZ, Lower Hutt, New Zealand

*Correspondence to*: Luc Beaufort (beaufort@cerege.fr)

**Abstract.** Automated analysis of calcareous nannofossils has progressively transformed coccolith-based paleoceanography by enabling the quantitative investigation of extremely abundant microfossil assemblages. Over the past three decades, the SYRACO (SYstème de Reconnaissance Automatique de COccolithes) framework evolved from one of the earliest neural-network–based recognition systems for micropaleontology into an integrated platform combining automated acquisition, object detection, morphometry and coccolith-mass estimation. Here, we retrace this methodological evolution from the first artificial neural networks developed in the 1990s to the current YOLOv8-based deep-learning framework.

We describe the successive developments in imaging, segmentation and object detection that improved over time coccolith recovery, quantitative robustness and operational scalability. Particular attention is given to the transition from segmentation-dependent workflows to integrated object detection, which fundamentally changed the balance between false positives and false negatives in quantitative coccolith analysis. To address the specific constraints of paleoceanographic applications, we use class-specific confidence thresholds to control inference reliability.

Beyond taxonomic recognition, the integration of bidirectional circular polarization imaging and automated morphometry progressively transformed SYRACO into a quantitative optical framework capable of estimating coccolith size, thickness and calcite mass on large datasets. As an illustration of the scientific applications enabled by these developments, we present a reanalysis of the EUMELI sediment-trap series from the Mauritanian upwelling system. This reanalysis reveals two short-lived coccolithophore export events during which *Emiliania huxleyi* and *Gephyrocapsa oceanica* dominated carbonate production and export, producing several grams of $CaCO_3$ $m^{-2}$ at 2500 m depth within about a month.

Together, these developments illustrate how successive generations of artificial intelligence and automated microscopy transformed coccolith analysis from a labor-intensive counting procedure into a scalable quantitative approach suitable for ecological, biogeochemical and paleoceanographic investigations.

https://doi.org/10.5194/egusphere-2026-3901
Preprint. Discussion started: 28 July 2026


## 1 1 Introduction

Calcareous nannofossils, the calcite plates produced by coccolithophores, are among the most abundant biogenic carbonate particles in the modern ocean and marine sediments (Milliman, 1993). Beyond their major importance for biostratigraphy (Berggren et al., 1985), coccolithophores play a fundamental role in marine biogeochemical cycles through the production and export of particulate inorganic carbon (PIC) (Hopkins et al., 2015; Balch et al., 2018; Ziveri et al., 2025). Variations in coccolith assemblages, morphology and calcification therefore provide valuable information on past ocean productivity (Beaufort et al., 1997; Hernández-Almeida et al., 2019), ecological dynamics (Okada and Mcintyre, 1979; Beaufort and Heussner, 2001; Guerreiro et al., 2017), carbonate chemistry (Poulton et al., 2007; Beaufort et al., 2011; Bach et al., 2012) and climate variability (Winter et al., 2014; Balch, 2018). Yet, despite their abundance and importance, quantitative investigation of coccolith assemblages has long remained constrained by the limitations of manual microscopy.

Traditional coccolith analysis relies on labor-intensive counting and taxonomic identification under the microscope, limiting both the number of analyzed specimens and the reproducibility of assemblage measurements. More importantly, manual approaches rarely provide easy access to quantitative information beyond relative abundance, because coccolith size, thickness and calcite mass are difficult to measure routinely at large scale, despite their recognized importance for coccolithophore ecology, calcification and paleoceanographic reconstructions (Bollmann et al., 2002; Henderiks, 2008; Young and Ziveri, 2000). As a consequence, coccolith assemblages have often remained primarily taxonomic datasets, whereas their potential for investigating calcification and carbonate export has remained only partially exploited.

To overcome these limitations, we initiated in the mid-1990s one of the earliest attempts to apply artificial neural networks to micropaleontology, leading to the development of SYRACO (SYstème de Reconnaissance Automatique de COccolithes) (Dollfus and Beaufort, 1999). From its inception, SYRACO followed an unusual strategy: rather than relying on predefined morphometric descriptors, the system was designed to learn directly from images, allowing automated recognition to adapt to the high morphological variability and optical complexity of coccoliths.

Since its first paleoceanographic applications (Beaufort et al., 2001), SYRACO evolved far beyond a simple recognition tool. Advances in microscopy, optical acquisition, automated image analysis and artificial intelligence gradually transformed the framework into an integrated quantitative platform combining object detection, morphometry and calcite-mass estimation (Beaufort, 2005; Beaufort et al., 2008; Beaufort et al., 2011). In particular, developments in advanced polarization imaging (Fuertes et al., 2014; Beaufort et al., 2014; Bollmann, 2014) made it possible to derive coccolith thickness and calcite mass from optical measurements. The later development of Bidirectional Circular Polarization (BCP) fundamentally improved this approach by making thickness estimates independent of incident light intensity and microscope-specific illumination settings. By relying on the ratio between opposite circular polarization states, BCP produces images in which signal intensity is linearly proportional to calcite thickness rather than illumination conditions, thereby enabling robust, reproducible and transferable thickness measurements across microscopes and acquisition systems (Beaufort et al., 2021).

https://doi.org/10.5194/egusphere-2026-3901
Preprint. Discussion started: 28 July 2026


More recently, deep-learning approaches based on YOLO object detection (Redmon et al., 2016) enabled large-scale automated quantification of individual coccoliths directly from microscope images. Combined with previous advances in polarization imaging, thickness estimation and calcite-mass quantification, this new generation of automated detection opened new opportunities for investigating coccolith assemblages. Rather than providing only abundance estimates, automated workflows now make it possible to reconstruct taxonomically resolved carbonate production and export, opening new perspectives for investigating links between plankton ecology, calcification and the marine carbon cycle.

In this article, we retrace the evolution of SYRACO over the past three decades, from its earliest neural-network implementations to the current deep-learning framework. We describe how successive developments in imaging, segmentation, object detection and optical quantification transformed coccolith analysis from a recognition problem into a scalable quantitative approach. Finally, we revisit the EUMELI sediment-trap series from the Mauritanian upwelling system (Morel, 1996), previously used as a benchmark dataset for SYRACOv3 validation (Beaufort and Dollfus, 2004a), to illustrate how three decades of developments now allow coccolith assemblages to be reinterpreted as quantitative carbonate-flux datasets rather than taxonomic counts alone.

## 2 SYRACO evolution

### 2.1 Early developments of SYRACO

When we first attempted automated coccolith recognition in the mid-1990s, both microscopy hardware and computing resources imposed severe constraints. Digital cameras were limited to 756×582 pixels with 8-bit depth, and processing capabilities were modest. To keep computation times manageable, we initially used a 50× objective instead of the standard 100×, reducing image size at the expense of spatial resolution (Table 1). These choices contrasted with alternative developments emerging at the same period, such as the Computer Guided Nannofossil Identification System (COGNIS) developed at ETH Zürich, which favored higher-resolution imaging and more computationally demanding segmentation workflows (Bollmann et al., 2004).

Despite these limitations, the optical properties of coccoliths provided a key advantage. Under crossed polarizers, calcite birefringence produces bright signals against a dark background, allowing efficient detection of coccoliths while excluding most non-birefringent particles such as quartz or biogenic silica. This natural contrast made coccoliths particularly well suited to early computer vision approaches.

At the time, most pattern recognition methods relied on handcrafted feature extraction, using descriptors such as shape parameters, Fourier transforms, or texture metrics. However, these approaches proved difficult to apply to coccoliths, whose morphology is highly variable and often affected by fragmentation, aggregation, or imaging artefacts. For this reason, SYRACO followed a different strategy: rather than defining explicit descriptors, the system was designed to learn features directly from pixel data (Dollfus and Beaufort, 1999).

https://doi.org/10.5194/egusphere-2026-3901
Preprint. Discussion started: 28 July 2026


The first neural network implemented in SYRACO operated on normalized 64×64 pixel images, after basic correction for translation and rotation. In modern terms, this architecture can be described as a multilayer perceptron with local receptive fields but without weight sharing. While simpler than later convolutional neural networks, it followed a similar rationale to early neural-network approaches to image recognition (e.g. Le Cun et al., 1990), although developed independently and with different architectural choices.

Trained on a dataset of coccolith and non-coccolith images, the system achieved about 86% classification accuracy across multiple taxa. More importantly, it demonstrated that neural networks could capture coccolith morphology directly from images, without relying on predefined measurements. From the outset, SYRACO was conceived as an operational system rather than a standalone classifier: detections were displayed in real time on microscope images, counted automatically, and stored as cropped images organized by class.

The first large-scale application of SYRACO was published in *Science* (Beaufort et al., 2001), marking the transition from a methodological prototype to a tool usable in routine paleoceanographic analyses.

This early phase of SYRACO established several key principles that remain central today: direct learning from images, robustness to morphological variability, and integration of detection, classification, and data storage within a single workflow. However, an important limitation remained: although classification accuracy was already high, a significant fraction of coccoliths present in a field of view was not detected, highlighting the need for improved recognition strategies.

| Year | Version | Objective (magnification) | Sensor resolution | Pixel size (µm) | Camera bit depth | Polarisation | Focus | Slide preparation method | Pattern recognition | Precision |
|---|---|---|---|---|---|---|---|---|---|---|
| **1996** | SYRACO v2 | 50X | 0.5 MP | 0.16 µm | 8 bits | Linear | Auto | Smear slides | CNN | 0.85 |
| **2004** | SYRACO v3 | 50X | 0.5 MP | 0.16 µm | 8 bits | Linear | Auto | Smear slides | Dyn CNN + hierarchical classifier | 0.91 |
| **2012** | SYRACO v3.1 | 100X | 4 MP | 0.062 µm | 14 bits | Linear | Auto | Smear slides | Dyn CNN + hierarchical classifier | |
| **2014** | SYRACO v4 | 100X | 4 MP | 0.062 µm | 14 bits | Rotative / circular | Auto | Random settling | Dyn CNN + Random Forest | 0.95 |
| **2020** | SYRACO v4.1 | 100X | 4 MP | 0.059 µm | 16 bits | BCP | Multi-focus | Random settling 8 mini-cover slips | ResNet50 | |
| **2024** | SYRACO v5 | 100X | 4 MP | 0.059 µm | 16 bits | BCP | Multi-focus | Random settling 8 mini-cover slips | YOLO v8 | 0.96 |

**Table 1: Evolution of the SYRACO system in the last 30 years.**

### 2.2 Technological maturation of SYRACO (2010s)

During the 2010s, several technological developments transformed SYRACO from a recognition tool into a quantitative platform for coccolith analysis (Table 1).

On the optical side, the return to 100× objectives, high-resolution low-noise cameras, and the development of advanced polarization methods considerably improved image quality. The introduction of three-polarizer imaging removed the

https://doi.org/10.5194/egusphere-2026-3901
Preprint. Discussion started: 28 July 2026


classical black cross associated with crossed polarizers, while later circular-polarization methods produced artifact-free coccolith images without radial optical extinction patterns (Beaufort et al., 2014). Finally, Bidirectional Circular Polarization (BCP) transformed image brightness into a quantitative proxy for calcite thickness independent of illumination conditions (Beaufort et al., 2021).

At the same time, segmentation and image-processing workflows evolved considerably. Early threshold-based approaches were gradually replaced by more robust pipelines combining background correction, contrast enhancement, watershed separation and morphometric filtering. Although increasingly reliable, these segmentation procedures remained computationally expensive and required extensive parameter tuning.

The software architecture also evolved toward fully automated acquisition. The transition to LabVIEW and NI Vision enabled synchronized microscope control, automated scanning, standardized image preprocessing, and automatic reconstruction of multifocus composite images, allowing routine unattended acquisition of up to 16 slides in a single batch. At the same time, the analytical capabilities of SYRACO continued to expand. The system was extended beyond individual coccolith recognition to include coccosphere analysis (Beaufort et al., 2008), while ensemble strategies combining neural networks with complementary classifiers such as Random Forests further improved classification robustness (Barbarin, 2014; Beaufort et al., 2022).

These developments progressively transformed SYRACO from a recognition tool into a quantitative analytical framework: automated recognition was complemented by morphometric measurements, coccosphere analysis, and optical estimates of coccolith thickness and calcite mass, thereby paving the way for modern deep-learning approaches.

### 2.3 Transition to integrated deep-learning frameworks

By the end of the 2010s, the historical SYRACO framework had reached intrinsic limits despite its robustness and widespread use in palaeoceanography. Its architecture relied on a multi-step pipeline combining preprocessing, segmentation, cropping, morphometric analysis, and classification. While effective, this design became increasingly inefficient as acquisition systems improved and datasets grew in size and complexity.

In particular, the segmentation step remained a critical bottleneck. The successive generation of large numbers of cropped images, followed by their transfer, storage, and classification, resulted in a processing chain that was slower than image acquisition itself. As microscope automation progressed, this imbalance became more pronounced: data production outpaced processing capacity. This limitation made clear that further improvements in classification accuracy alone would not be sufficient, and that the structure of the pipeline itself needed to be reconsidered.

Initial experiments with modern convolutional neural networks (CNNs), particularly residual architectures such as ResNet50 (He et al., 2016), confirmed that more recent models could significantly improve classification accuracy and reduce false positives. However, these approaches still relied on pre-segmented and cropped images, and therefore did not address the fundamental limitations of the SYRACO pipeline.

https://doi.org/10.5194/egusphere-2026-3901
Preprint. Discussion started: 28 July 2026


A major shift occurred with the adoption of object-detection frameworks, in particular the YOLO (You Only Look Once) family of algorithms (Redmon et al., 2016). Unlike traditional approaches based on separate segmentation and classification steps, YOLO integrates detection and classification within a single architecture. In this framework, coccoliths are directly localized and classified from raw microscope images, eliminating the need for intermediate segmentation and substantially reducing computational overhead.

For SYRACO, this integration addressed two major challenges simultaneously: it removed the computational bottleneck associated with segmentation and image handling, enabling near real-time processing of microscope fields, while also improving robustness by reducing false positives. More fundamentally, this transition marked a shift from a sequential pipeline composed of multiple independent processing steps to a fully integrated system performing detection and classification directly on raw images.

## 3 Current SYRACO description

### 3.1 Automated image acquisition

The transition from SYRACOv2 to SYRACOv5 (Fig. 1) reflects much more than an increase in image resolution. Early SYRACO images mainly contained shape information, with strong contrast enhancement compensating for the limited spatial resolution and dynamic range imposed by the computing resources available in the 1990s. In contrast, modern SYRACO images contain substantially richer information, including continuous birefringence gradients, internal texture, and quantitative variations in calcite thickness. This evolution fundamentally changed the type of information available for automated recognition and strongly contributed to the efficiency of modern deep-learning approaches.

https://doi.org/10.5194/egusphere-2026-3901
Preprint. Discussion started: 28 July 2026


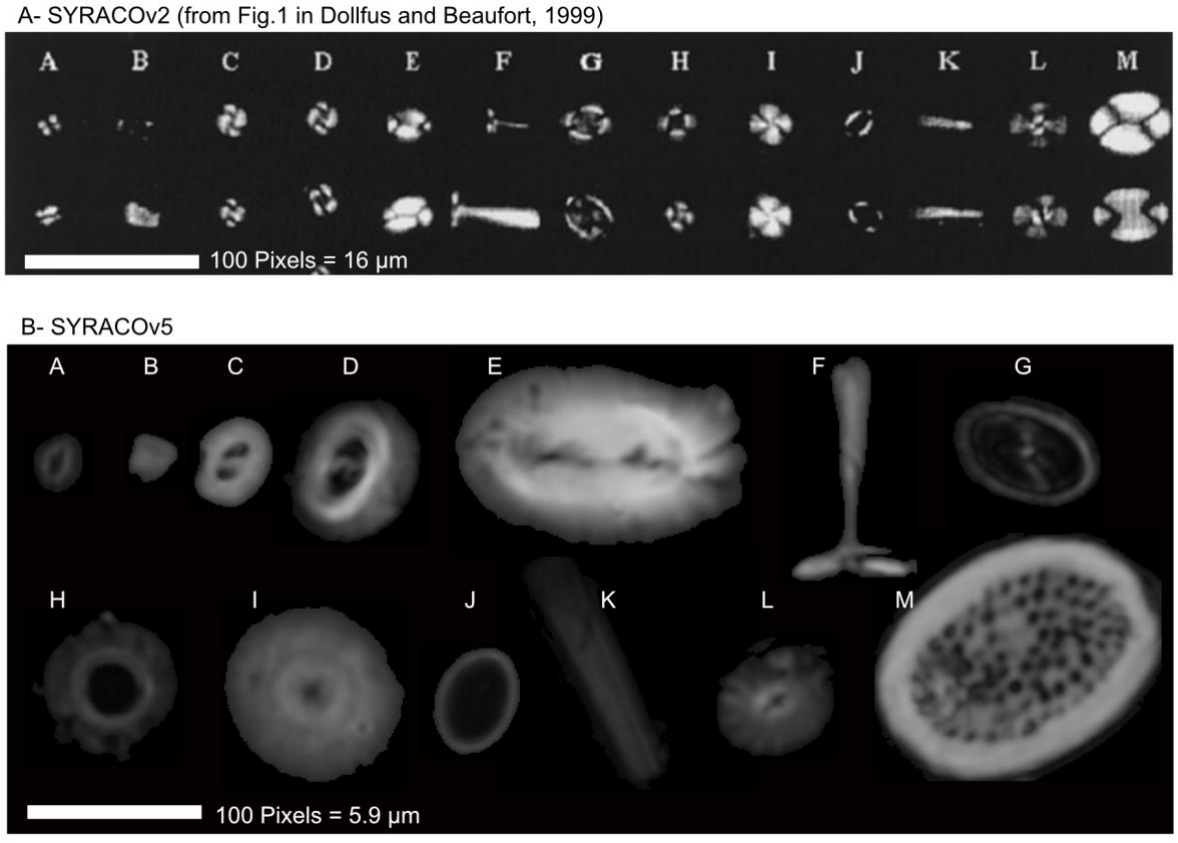


**Figure 1: Evolution of image quality from SYRACOv2 to SYRACOv5. (A) Two examples for each coccolith class used in SYRACOv2, cropped from Figure 1 of Dollfus and Beaufort (1999). (B) Representative examples of the same classes extracted from the SYRACOv5 training set. White bars indicate the scale in pixels and the corresponding equivalent size in micrometers for each panel. In the early SYRACO versions, computer limitations constrained image resolution, making shape a more important feature than texture for automated recognition. Images were therefore intentionally contrast-enhanced. The black cross visible in the upper images results from linear polarization microscopy. The lower images were acquired using Bidirectional Circular Polarization (BCP), which suppresses the black cross and produces images in which brightness is linearly related to calcite thickness. A, *Emiliania huxleyi*; B, *Florisphaera profunda*; C, *Gephyrocapsa caribbeanica*; D, *Gephyrocapsa oceanica*; E, *Helicosphaera carteri*; F, *Rhabdosphaera* spp.; G, *Syracosphaera pulchra*; H, *Umbilicosphaera sibogae*; I, *Calcidiscus leptoporus*; J, *Syracosphaera* spp.; K, *Gladiolithus flabellatus*; L, *Umbellosphaera tenuis*; M, *Pontosphaera* spp.**

A major step in this transition was the progressive replacement of classical crossed linear polarization by Bidirectional Circular Polarization (BCP) (Fig. 1). In early systems, birefringent coccoliths displayed a characteristic black cross, creating abrupt extinction patterns that partially masked morphological details. BCP suppresses this artifact and produces images in which brightness varies continuously with calcite thickness. By combining paired images acquired under opposite circular polarization states, coccolith thickness can be estimated through a simple optical relationship, transforming the image from a primarily morphological representation into a quantitative map of calcite distribution.

https://doi.org/10.5194/egusphere-2026-3901
Preprint. Discussion started: 28 July 2026


At the same time, improvements in acquisition hardware considerably enhanced image fidelity. Modern SYRACOv5 systems operate on Leica DM6000 B and DM6 B microscopes equipped with 100× oil-immersion objectives and high-resolution low-noise digital cameras (14–16 bit depth). Multifocus acquisition is systematically used to compensate for uneven specimen topography. Each field of view is acquired as a z-stack spanning several focal depths, and a hyperfocal algorithm reconstructs an all-in-focus composite image by selecting the sharpest regions for each focal depth. This procedure preserves fine coccolith structures over the entire field while improving the consistency of image features used for recognition.

Image acquisition is fully automated by the CoccoSnail system. Cover slips are scanned along spiral trajectories through contiguous fields of view (~125 × 125 µm), with focus initialization propagated from one field to the next to optimize acquisition speed and stability. Depending on sample density and acquisition settings, hundreds of contiguous fields can be recorded automatically for a single sample.

Together, BCP imaging, multifocus reconstruction, high-dynamic-range acquisition, and automated scanning transformed the nature of coccolith images used by SYRACO (Fig. 1). Rather than relying mainly on silhouettes and contrast-enhanced outlines, SYRACOv5 operates on quantitatively consistent, information-rich images containing stable morphological and optical features. These improvements provide the high-quality input required for direct object detection and classification using modern deep-learning frameworks such as YOLO.

### 3.2 Training sets construction

A major obstacle for training object-detection models on coccolith assemblages is the extreme imbalance of natural populations. In typical microscope fields, a few dominant taxa account for most individuals, whereas many morphotypes occur at frequencies well below 1%. Under such conditions, obtaining sufficiently large annotated datasets for rare taxa would require the manual annotation of millions of coccoliths, making conventional training strategies impractical.

To overcome this limitation, we adopted a fundamentally different approach based on the generation of synthetic coccolith assemblages. Instead of manually annotating natural microscope fields, we constructed artificial fields by inserting real coccolith images into empty microscope backgrounds. This strategy allowed us to generate balanced training datasets while preserving realistic object textures, optical properties, and size distributions.

The synthetic assemblages were generated from existing image libraries initially developed for ResNet50 training (SYRACOv4.1). These libraries contained cropped coccoliths representing 28 morphotypes selected to provide a generalized representation of Plio–Pleistocene assemblages while remaining applicable to older intervals, at least back to the Miocene (Fig.2). The overall strategy intentionally favored “lumping” rather than strict taxonomic splitting, with the objective of producing a robust detection model capable of recognizing most major coccolith morphologies encountered in natural samples. This generalized framework can subsequently support more specialized secondary classifiers in hierarchical pipelines, following principles already explored in earlier SYRACO versions (Beaufort and Dollfus, 2004a).

https://doi.org/10.5194/egusphere-2026-3901
Preprint. Discussion started: 28 July 2026


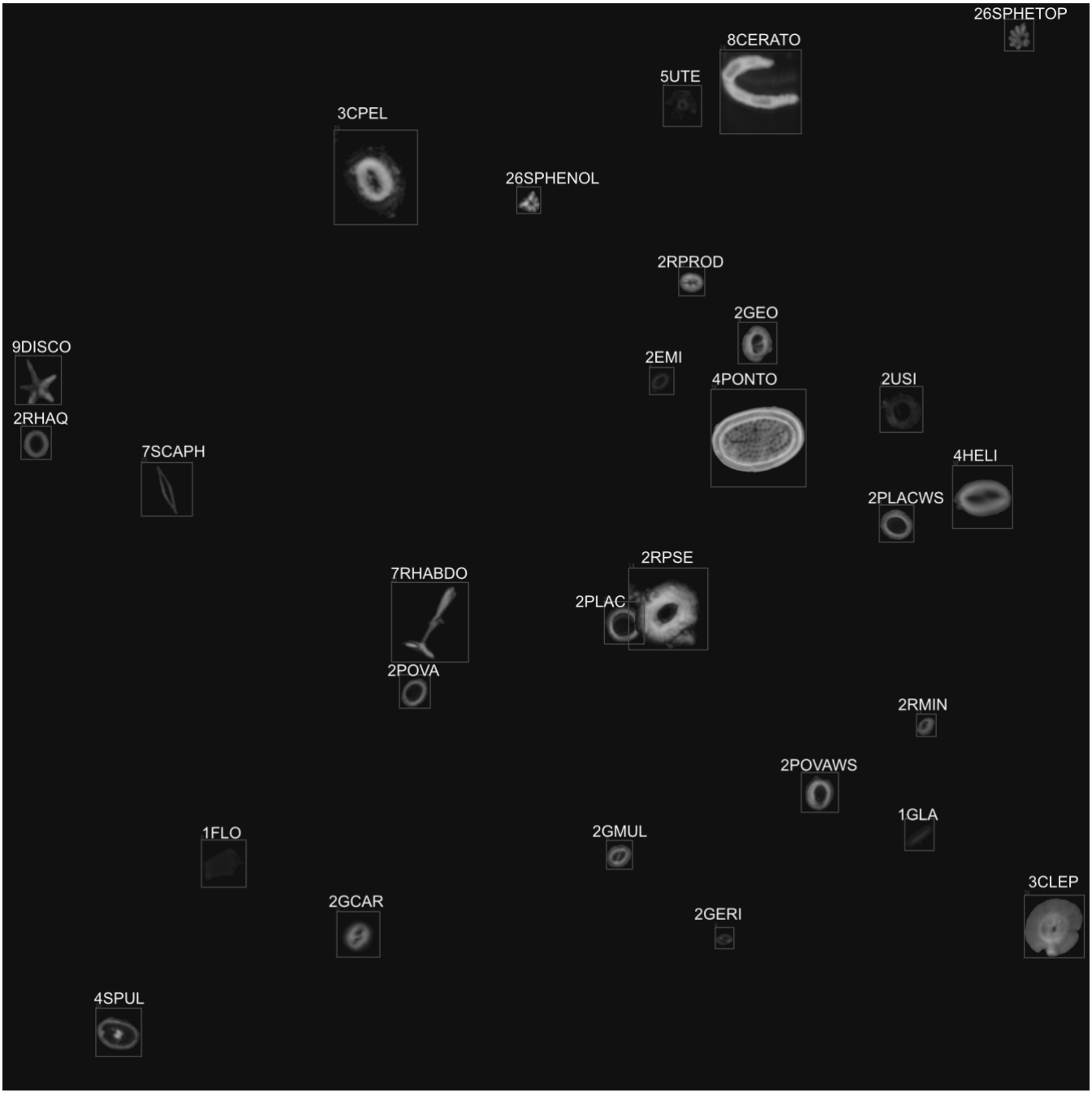


220 **Figure 2. Example of a synthetic training image used for YOLOv8 training. Bounding boxes from annotations are shown in gray and labels indicate the operational classes used during training and inference. Classes are grouped by major coccolithophore taxa and correspond to image-based morphotypes targeting representative species rather than formal taxonomic determinations. The correspondence between class labels and representative species is provided in Table A1.**

https://doi.org/10.5194/egusphere-2026-3901
Preprint. Discussion started: 28 July 2026


An exception was made for the Noelaerhabdaceae family, for which a deliberately fine-grained strategy was adopted. This family is characterized by extreme morphological plasticity and overlapping size-defined morphotypes. Rather than simplifying this variability, we chose to preserve it by defining 13 partially overlapping classes. The objective was not to enforce rigid taxonomic boundaries, but to expose the neural network to the full phenotypic continuum of the group, allowing later regrouping of morphotypes depending on the scientific objectives of each study.

A custom script was developed to generate synthetic microscope fields of 2048 × 2048 pixels, corresponding to the dimensions of standard acquisition images. Cropped coccoliths were randomly distributed within these fields while preventing object overlap. Because the exact coordinates of each inserted object were known, annotation files in YOLO format could be generated automatically without manual labeling. Approximately 300 instances of each class were distributed across 300 synthetic images, producing balanced assemblages in which all morphotypes were equally represented despite their very different abundances in nature.

This strategy shifted the training process from exhaustive annotation of natural assemblages to the controlled generation of synthetic ecological communities. It provided several major advantages: balanced class representation, preservation of realistic coccolith appearance, automatic annotation generation, and efficient training on rare morphotypes without requiring prohibitively large manually annotated datasets.

The final dataset was divided into training, validation, and test subsets (240, 30, and 30 images per class, respectively). In addition, 30 natural microscope images devoid of coccoliths were included as negative examples to improve the ability of the network to distinguish true coccoliths from contaminants and background structures.

### 3.3 YOLOv8 training

YOLOv8 models were trained using the synthetic coccolith assemblages described above. Among the tested architectures, YOLOv8m provided the best compromise between detection accuracy, robustness, and computational cost, and was therefore selected for this study. Training was performed within the Ultralytics framework using transfer learning from pretrained weights. Standard augmentation procedures (rotations, scaling, contrast variations, mosaic augmentation) were applied to increase robustness to natural variability in coccolith orientation, preservation state, and illumination conditions.

The inclusion of negative images devoid of coccoliths proved important for limiting false positives generated by contaminants, background structures, or optical artefacts. For birefringent coccoliths, training and validation losses decreased steadily and converged after approximately 150 epochs, with no indication of overfitting. Precision, Recall, and mAP values all exceeded 0.9, indicating stable convergence and robust object-detection performance. The normalized confusion matrix (Fig. 3) confirms the high classification reliability of the YOLOv8m model across the 28 morphotypes used in this study. Most residual confusions are restricted to morphologically similar taxa, particularly within the Noelaerhabdaceae, where several morphotypes differ primarily by size or by subtle optical traits approaching the limits of optical microscopy resolution.

https://doi.org/10.5194/egusphere-2026-3901
Preprint. Discussion started: 28 July 2026


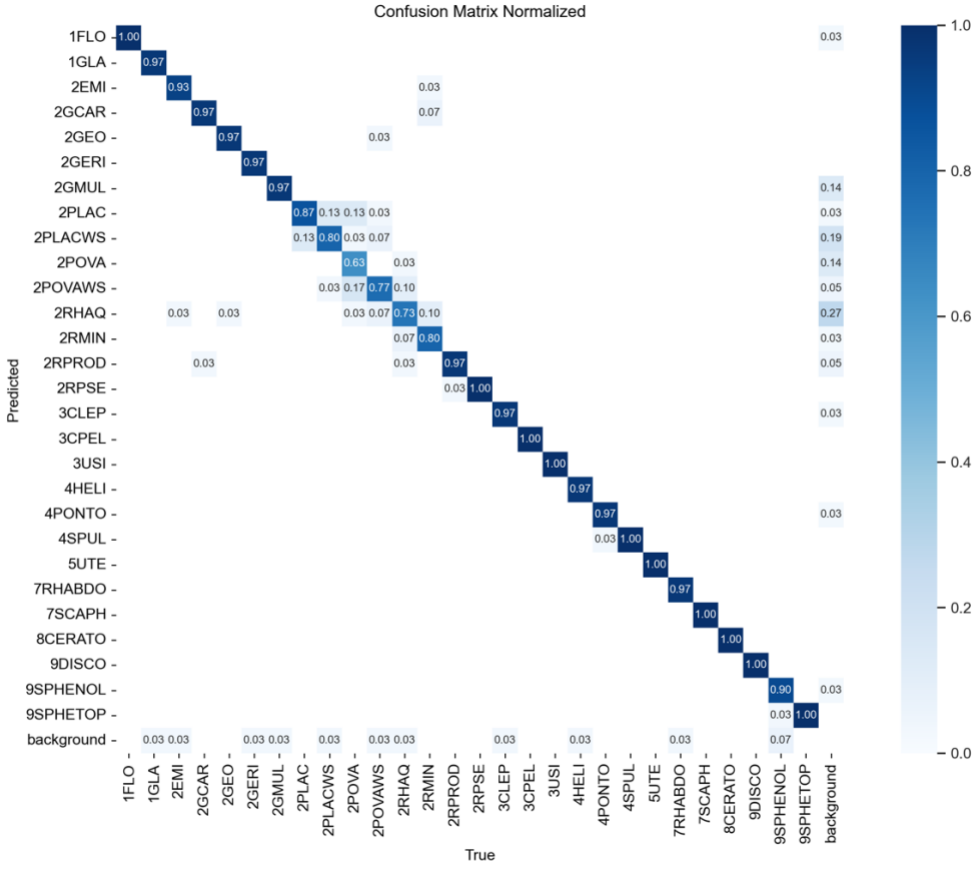


**Figure 3: Normalized confusion matrix showing the classification performance of the YOLOv8m model across the 28 operational morphotypes illustrated in Figure 2. Diagonal values represent correctly classified individuals. Off-diagonal elements indicate misclassifications, which remain low and mostly occur among closely related or morphologically similar taxa, such as within the Noelaerhabdaceae group (labels starting with "2") or between *Pontosphaera* and *Syracosphaera*. Overall, accuracy exceeds 0.9 for most classes and reaches 0.98 when operational classes (e.g. 2PLAC and 2PLACWS) and morphologically similar Noelaerhabdaceae taxa are lumped. Class labels and representative species is provided in Table A1**

Model performance was evaluated using Recall and Precision. Interpretation of these metrics is nevertheless influenced by the deliberately overlapping Noelaerhabdaceae classes used during training. Because these classes were designed to sample the full phenotypic continuum of the group, some apparent misclassifications reflect transitions between neighboring morphotypes rather than true recognition failures (Fig. 3). When such confusions were not penalized, mean Recall increased from 0.93 to 0.98 and mean Precision from 0.91 to 0.96.

Although confusion-matrix metrics (Precision, Recall, mAP) remain useful indicators of detection performance, they are influenced by dataset composition and do not necessarily reflect performance on natural assemblages. The ability of the model to generalize to natural coccolith communities is therefore evaluated independently in Section 4.

https://doi.org/10.5194/egusphere-2026-3901
Preprint. Discussion started: 28 July 2026


### 3.4 Automated inference workflow

During inference, raw microscope fields are processed directly by the trained YOLOv8 network, which simultaneously localizes and classifies coccoliths without requiring prior segmentation. Detected objects are automatically cropped and stored by predicted class, while abundance tables are generated in parallel. Depending on the acquisition mode, the system additionally extracts morphometric and optical measurements for each detected individual, including coccolith length, width, thickness, and calcite mass. Annotated images with superimposed bounding boxes and class labels can also be generated for visual inspection and quality control.

This integrated workflow represents a major simplification compared with earlier SYRACO generations, which relied on sequential pipelines involving segmentation, object extraction, transfer of cropped images, and secondary classification steps. By combining localization and classification within a single framework, YOLOv8 strongly reduces computational bottlenecks while improving the consistency of object detection.

However, quantitative micropalaeontological inference requires more than object detection alone. The practical challenge lies in controlling how recognition errors propagate to assemblage reconstruction. In particular, reliable paleoceanographic applications require minimizing both the artificial inflation of assemblages through erroneous detections and the loss of genuine coccolith information.

### 3.5 Detection integrity and uncertainty in quantitative inference

Evaluating inference quality in quantitative micropaleontology requires more than conventional deep-learning metrics alone. Metrics such as Precision, Recall, or mAP do not distinguish between two fundamentally different types of errors: (i) the artificial inflation of assemblages by false positives, and (ii) the loss of genuine coccoliths through failed detection. From a paleoceanographic perspective, these two errors have very different consequences. False positives introduce spurious abundance signals, whereas undetected coccoliths irreversibly remove information from the assemblage.

Importantly, false positives in coccolith recognition are not solely composed of random hallucinations or unrelated background particles. A substantial fraction corresponds to biologically meaningful but taxonomically invalid objects, including broken coccoliths, overlapping specimens, and especially coccolith aggregates. For example, in sediment-trap material, aggregates of abundant morphotypes may recurrently mimic rarer taxa. Such detections often remain visually plausible and may even receive moderate confidence scores, making confidence-based uncertainty estimates alone insufficient for quantitative paleoecological applications.

Historically, false positives represented the dominant limitation of earlier SYRACO generations (Beaufort and Dollfus, 2004b), motivating the development of successive correction strategies including secondary classifiers, geometric compatibility filters, and ensemble approaches. Although these developments substantially reduced background invasion, residual inference errors remain morphotype dependent.

https://doi.org/10.5194/egusphere-2026-3901
Preprint. Discussion started: 28 July 2026


For this reason, detections are not validated using a single global confidence threshold. Instead, class-specific thresholds (τ) are determined independently for each morphotype.

To estimate these thresholds, a limited number of representative validation samples are first selected. Within these samples, all objects detected above a low confidence level (0.05) are retained together with their associated confidence values. Detections are subsequently examined by a specialist and separated into true positives and false positives for each class. The distributions of true-positive and false-positive detections are then calculated as a function of confidence level.

Figure 4 illustrates this procedure for two representative morphotypes (1FLO and 2EMI) using the same EUMELI samples previously analyzed in Beaufort and Dollfus (2004), reprocessed here using the settling preparation method because the original slides were no longer available. The optimal threshold τ is defined empirically as the value minimizing false positives while preserving the highest possible number of true positives. Because the balance between these two error types differs substantially among coccolith morphotypes, class-specific thresholds provide a more robust strategy than the use of a single global confidence threshold.

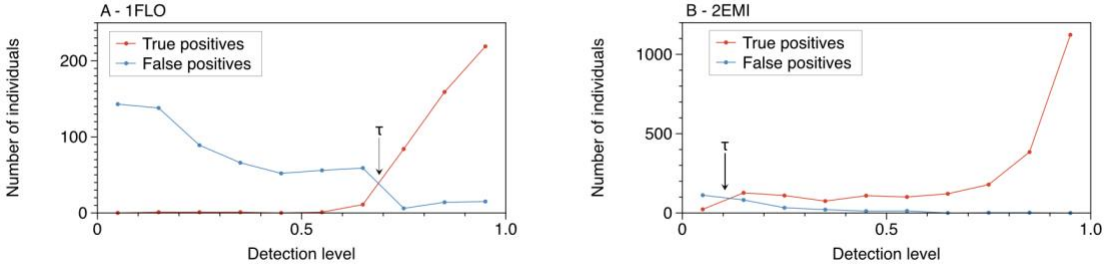


**Figure 4: Class-specific detection levels calculated from three pooled EUMELI samples (EUMELI II2M-2, -3, -4) for the SYRACOv5 classes 1FLO (A) and 2EMI (B). True positives are shown in red and false positives in blue. The arrow labelled τ indicates the optimal detection threshold.**

Under these conditions, residual inference errors are largely restricted to biologically meaningful ambiguities between closely related morphotypes rather than failures of object localization. In practice, optimized thresholds are determined on validation subsets and subsequently fixed for operational analyses, ensuring reproducibility and comparability across datasets.

## 4 Routine work evaluation

The ultimate evaluation of an automated micropalaeontological workflow is not limited to benchmark metrics computed on synthetic datasets, but to its capacity to preserve ecologically meaningful assemblage signals during routine operation.

To evaluate this aspect, we compared SYRACOv5 results with historical SYRACO analyses and human counts using sediment-trap samples from the French JGOFS EUMELI program off Senegal. These samples were previously used for the

https://doi.org/10.5194/egusphere-2026-3901
Preprint. Discussion started: 28 July 2026


operational evaluation of SYRACOv3 (Beaufort and Dollfus, 2004), providing a unique benchmark for assessing the long-term evolution of the system under real working conditions.

The first three EUMELI samples were reprocessed using the modern settling preparation method combined with ultrasonication, since the original smear slides were no longer available. Detection results obtained by SYRACOv3, SYRACOv5, and human counting can therefore be directly compared.

Figure 5 shows that assemblage-level abundance estimates remain highly consistent across successive SYRACO generations despite major differences in image acquisition, optical configuration, and inference strategies. The higher coccolith abundances detected by SYRACOv5 mainly reflect improved object recovery resulting from modern preparation and acquisition workflows. Ultrasonication breaks coccolith-rich aggregates that previously masked undetected individuals, higher-resolution imaging improves the visibility of small coccoliths, multifocus reconstruction maintains all objects in focus simultaneously, and Bidirectional Circular Polarization suppresses orientation-dependent extinction effects that previously obscured some morphotypes such as *Florisphaera profunda*.

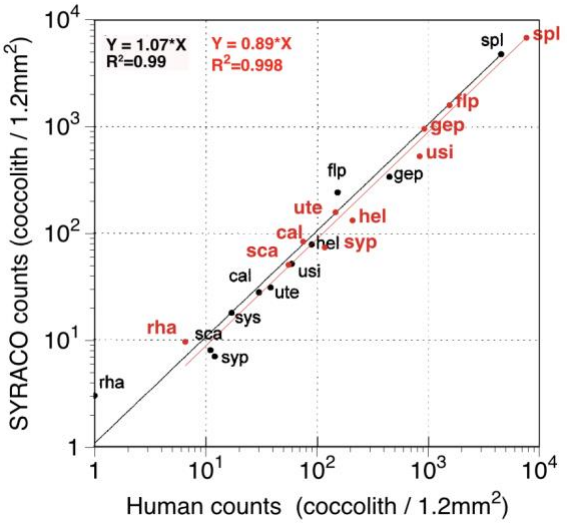


**Figure 5: Comparison of human counts and SYRACO counts in three EUMELI samples (EUMELI II2M-2, -3, -4). Red: SYRACOv5; black: SYRACOv3 (from Figure 5 in Beaufort and Dollfus, 2005). SYRACOv5 density counts were adjusted to match those of SYRACOv3, allowing direct comparison with the 2004 dataset**

Importantly, these technological improvements primarily affect the recovery of genuine coccoliths rather than the ecological structure of the assemblages themselves. Despite substantial changes in hardware and inference architecture over the last three decades, the main abundance relationships remain highly conserved, demonstrating the long-term robustness of the SYRACO framework.

https://doi.org/10.5194/egusphere-2026-3901
Preprint. Discussion started: 28 July 2026


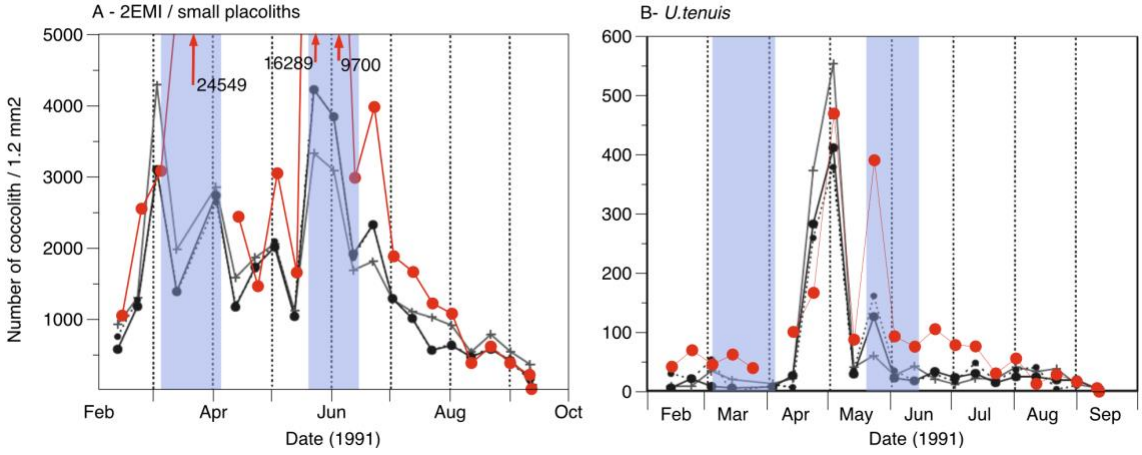


**Figure 6 : Comparison of coccolith detection by SYRACOv3 and SYRACOv5 from the EUMELI IIM sediment-trap series off Cap Blanc (West Africa). Background black curves are adapted from Figure 7 in Beaufort and Dollfus (2004), showing SYRACOv2 corrected counts (solid lines with closed circles) and human counts (crosses). Red curves show SYRACOv5 counts. Vertical bluish-grey bands indicate the timing of two phytoplankton blooms (Bory et al., 2002). Coccolith-rich aggregates, which are important during these blooms, were broken by ultrasonication during sample preparation for SYRACOv5, likely explaining the higher coccolith counts obtained during these two events. (A) Results for *Emiliania huxleyi* and small *Gephyrocapsa* grouped together. (B) Results for *Umbellosphaera tenuis*.**

This robustness is also visible at the temporal scale of complete sediment-trap series.

Figure 6 compares coccolith flux reconstructions obtained by SYRACOv3 and SYRACOv5 over the EUMELI III-M sediment-trap time series. The major ecological structures of the signal, including the timing of phytoplankton blooms and the relative temporal variations of dominant taxa, are preserved across both generations of the system. SYRACOv5 nevertheless detects substantially larger coccolith abundances during bloom periods, largely because modern preparation procedures recover coccoliths that previously remained hidden within aggregates.

Together, these comparisons demonstrate that the historical evolution of SYRACO shifted the dominant source of error from false-positive contamination toward near-exhaustive object recovery. In SYRACOv5, remaining uncertainties are now largely confined to taxonomic ambiguities among closely related morphotypes rather than failures of detection itself. This transition is critical for quantitative micropaleontology, where preserving the integrity of abundance signals is more important than achieving perfectly discrete taxonomic classification.

## 5 Scientific applications and perspectives

### 5.1 Examples from literature

The developments described above enabled a broad range of quantitative paleoceanographic applications. Automated coccolith assemblage analysis made it possible to reconstruct changes in productivity, nutricline dynamics and upper-ocean structure linked to ENSO-like variability, monsoon systems and orbital forcing (e.g. Beaufort et al., 2001; Beaufort et al.,

https://doi.org/10.5194/egusphere-2026-3901
Preprint. Discussion started: 28 July 2026


2010; Bolliet et al., 2011; Ivanova et al., 2012; Staines-Urías et al., 2015; Su et al., 2013; Le Mézo et al., 2017). By considerably increasing the number of counted specimens and analyzed samples, automated workflows also enabled statistically robust reconstructions of seasonal to interannual climate variability from laminated sediments, including ENSO and Pacific Decadal Oscillation (PDO) dynamics over extended time periods (Grelaud et al., 2009a; Grelaud et al., 2009b; Beaufort and Grelaud, 2017). Similar advantages proved particularly valuable for the interpretation of long sediment-trap time series, where large numbers of observations are required to resolve rapid ecological fluctuations (Meier et al., 2014; Godbillot et al., 2025).

Beyond taxonomic assemblage analysis, the SYRACO framework increasingly evolved into a quantitative morphometric and optical system capable of estimating coccolith size, thickness and calcite mass. These developments enabled quantitative investigations of coccolith dissolution (Beaufort et al., 2007), coccolithophore calcification and carbonate production (Beaufort et al., 2008; Kruijt et al., 2026), including studies of coccolith mass variability in culture experiments and across geological timescales (Beuvier et al., 2019; Mcclelland et al., 2016; Muller et al., 2012; Su et al., 2020; Valença et al., 2024). They also contributed to investigations of ocean acidification and carbonate chemistry (Engel et al., 2005; Beaufort et al., 2011), as well as to studies of the carbonate counter pump (Duchamp-Alphonse et al., 2018).

More recently, high-resolution morphometric datasets generated through automated coccolith analysis contributed to studies linking coccolithophore evolution to eccentricity-paced changes in tropical seasonality during the Pleistocene (Beaufort et al., 2022), illustrating how high-throughput coccolith analysis can now be used to investigate evolutionary responses to climate variability over orbital timescales.

Finally, the methodological framework initially developed for coccolith recognition is now being extended toward a broader family of specialized AI pipelines. These include workflows dedicated to coccospheres (Beaufort et al., 2008; Kruijt et al., 2026; Lassus et al., 2026), ancient coccolith assemblages (Suchéras-Marx et al., 2014), non-birefringent coccoliths (Beaufort et al., in prep.), as well as other siliceous and calcareous microplankton groups such as diatoms (Godbillot et al., 2024), pollen (Bourel et al., 2020; Gimenez et al., 2024), foraminifera (Marchant et al., 2020) and radiolarians (Tetard et al., 2020).

### 5.2 Application to sediment trap

As an illustration of the type of quantitative analyses enabled by automated coccolith recognition, the EUMELI sediment-trap series from the Mauritanian upwelling system was reanalyzed using coccolith assemblage composition and coccolith-mass estimates derived from SYRACO workflows. This site was chosen because it had already been investigated using an earlier generation of SYRACO (Beaufort and Dollfus, 2004a) allowing direct comparison between the type of analyses achievable at the time and those enabled by the present workflow (Figures 5 and 6). The EUMELI program (EUtrophic, MEsotrophic and oLIgotrophic), conducted within the framework of the France-JGOFS program (Joint Global Ocean Flux Study), aimed to investigate progressive changes in biogeochemical processes associated with the offshore dissipation of the Mauritanian upwelling and the resulting decrease in biological activity from productive coastal waters toward the subtropical gyre (Morel, 1996). The original study documented exceptionally large downward particle fluxes associated with episodic

https://doi.org/10.5194/egusphere-2026-3901
Preprint. Discussion started: 28 July 2026


offshore advection of productive upwelling filaments (Bory et al., 2001). In particular, two intense export events occurred in spring and early summer 1991, with estimated settling velocities exceeding 600 m $day^{-1}$ (Bory et al., 2001).

The SYRACO-based reanalysis focused on the sediment trap deployed at 2500 m depth during these two short-lived export events. Following the workflow described above, automated coccolith recognition combined with individual coccolith mass estimation yielded an estimated export of 3.1 g $CaCO_3$ $m^{-2}$ over the ~60 days encompassing the two major pulses (Figure 7). This value should be regarded as a conservative estimate of coccolith-derived carbonate export, because large coccolith-rich aggregates and fragmented coccolith debris—which may contribute substantially to the carbonate load—cannot be reliably quantified by the recognition system and are therefore excluded from the calculation.

Because carbonate mass is estimated at the level of individual coccoliths, this approach also makes it possible to resolve the taxonomic structure of carbonate export. During both export pulses, the Noelaerhabdaceae overwhelmingly dominated the coccolith carbonate flux, with *Emiliania huxleyi* and *Gephyrocapsa oceanica* accounting for most of the exported coccolith carbonate (Figure 7). Notably, the proportion of these taxa increased sharply during the two short-lived export events, indicating that intense episodic blooms may disproportionately contribute to deep-ocean carbonate transfer in mesotrophic upwelling systems.

These results illustrate how automated coccolith recognition combined with optical coccolith-mass estimation transforms coccolith assemblages from purely taxonomic datasets into quantitative carbonate-flux assemblages. The unusually high settling velocities reported by Bory et al. (2001) (>600 m $day^{-1}$) are consistent with the idea that coccolith-rich aggregates enhanced particle density and acted as mineral ballast, thereby accelerating export to the deep ocean. This example highlights how the evolution of SYRACO—from a recognition system toward an integrated morphometric and optical framework—opens new opportunities to investigate links between plankton ecology, calcification and the marine carbon cycle.

More fundamentally, this example illustrates how the scientific information extracted from the same samples has evolved over the past three decades. The very same sediment-trap samples that originally served to validate automated coccolith counting can now be reanalyzed to provide taxonomically resolved estimates of carbonate export, linking coccolith assemblages directly to biogeochemical fluxes. This progression illustrates that advances in artificial intelligence, quantitative optical microscopy and automated morphometry have not simply improved counting performance, but have considerably expanded the range of scientific questions that coccolith assemblages can address.

https://doi.org/10.5194/egusphere-2026-3901
Preprint. Discussion started: 28 July 2026


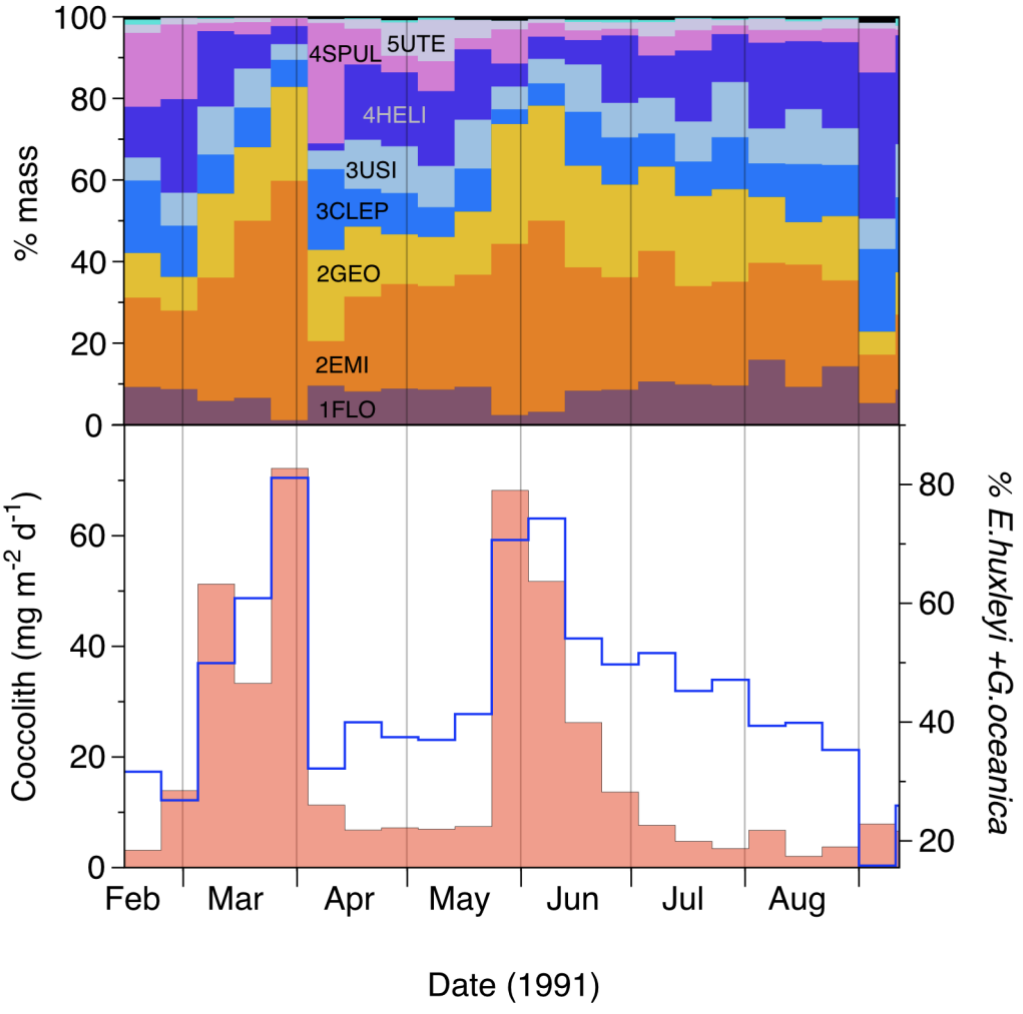


**Figure 7. Quantitative reanalysis of coccolith carbonate export during the EUMELI sediment-trap series (Mauritanian upwelling system, 1991) using the SYRACO workflow. Upper panel: temporal evolution of the taxonomic composition of coccolith carbonate export expressed as the percentage contribution of coccolith mass by species. Lower panel: estimated coccolith carbonate export (filled histogram, mg $m^{-2}$ $d^{-1}$) at 2500 m depth, derived from individual coccolith mass estimates obtained through automated recognition and bidirectional circular polarization measurements. The blue curve shows the relative mass contribution (%) of Noelaerhabdaceae (*Emiliania huxleyi* + *Gephyrocapsa oceanica*) to total coccolith carbonate export. Two major short-lived export events occurred in spring and early summer 1991, corresponding to episodic offshore advection of productive upwelling filaments (Bory et al., 2001).**

## 6 Conclusions

Over the past three decades, SYRACO has evolved from an early neural-network–based recognition system into a comprehensive framework for automated coccolith analysis. This evolution reflects not a single technological breakthrough, but the gradual convergence of advances in microscopy, image acquisition, optical quantification and machine learning.

https://doi.org/10.5194/egusphere-2026-3901
Preprint. Discussion started: 28 July 2026


Together, these developments have progressively removed some of the practical limitations that historically constrained coccolith analysis, particularly the time required for large assemblage counts and the difficulty of routinely extracting quantitative information beyond taxonomy.

A major consequence of this evolution is that coccolith assemblages can now be investigated not only in terms of taxonomic composition, but also through quantitative descriptors such as coccolith morphology, thickness and calcite mass. The integration of automated detection with optical measurements makes it possible to estimate taxonomically resolved carbonate standing stocks, export and burial, opening new opportunities for investigating the relationships between coccolithophore ecology, calcification and the marine carbon cycle. The introduction of class-specific detection thresholds (τ) further improved the reliability of quantitative assemblage reconstruction by minimizing false detections while preserving genuine coccolith diversity.

The EUMELI sediment-trap reanalysis illustrates the type of quantitative analyses that can now be achieved using automated coccolith workflows. Revisiting a dataset previously used to validate earlier SYRACO generations demonstrates how the same material can now be re-examined through quantitative carbonate estimates in addition to assemblage composition while preserving the main ecological structure of the original signal. At the same time, this case study also reflects a deliberate simplification of the present implementation. Coccolith aggregates and fragmented material, although previously quantified within the broader SYRACO framework and likely contributing substantially to carbonate export, were not included as dedicated training classes and were therefore excluded from carbonate estimates.

More broadly, the methodological framework initially developed for coccolith recognition is now being extended toward specialized workflows dedicated to coccospheres, ancient assemblages, non-birefringent coccoliths and other plankton groups. Rather than simply improving counting performance, successive developments have progressively expanded the information that can be extracted from coccolith assemblages, enabling quantitative investigations of morphology, calcification and carbonate fluxes in addition to taxonomic composition. Whether these developments ultimately transform routine micropalaeontological practice will depend not only on algorithmic performance, but also on their capacity to deliver robust and reproducible quantitative information across diverse ecological and paleoceanographic settings.

Beyond these methodological advances, automated coccolith analysis provides a powerful framework for biogeoscience applications. Automated quantification of coccolith assemblage composition, morphology and calcite mass enables large-scale investigations of plankton calcification, quantitative reconstruction of taxonomically resolved carbonate production through geological time, and improved assessments of the contribution of coccolithophores to the marine carbon cycle. Analyses of filtered surface-water samples now provide estimates of carbonate standing stocks associated with coccospheres and detached coccoliths (Kruijt et al., 2026), allowing haptophyte carbonate production to be quantified (Lassus et al., 2026). Applied to sediment traps and marine sediments, the same methodology provides species-specific carbonate export and long-term burial fluxes (e.g. Beaufort et al., 2022). By linking taxonomically resolved carbonate production, export and burial within a single analytical framework, SYRACO transforms automated coccolith analysis from a taxonomic tool into a quantitative approach for investigating the marine carbonate cycle.

https://doi.org/10.5194/egusphere-2026-3901
Preprint. Discussion started: 28 July 2026


## Appendix A

| Class label | Reference species (higher taxa in bold) | Complementary species | Diagnostic morphological features |
|---|---|---|---|
| | **Isochrysidales** | | |
| 2EMI | *Emiliania huxleyi* | *Reticulofenestra minuta*, *Gephyrocapsa ericsonii* | Small placolith with a dark distal shield and an open central area (*E. huxleyi* with a closed central area, type R, is included in class 2GCAR) |
| 2GCAR | *Gephyrocapsa caribbeanica* | *Reticulofenestra producta*, *Gephyrocapsa oceanica*, *Gephyrocapsa muellerae* | *Gephyrocapsa* with a small central area |
| 2GEO | *Gephyrocapsa oceanica* | *Gephyrocapsa caribbeanica*, *Reticulofenestra haqii* | Large *Gephyrocapsa* with a wide central area |
| 2GERI | *Gephyrocapsa ericsonii* | *Gephyrocapsa muellerae* | Small *Gephyrocapsa* with a distinct bridge |
| 2GMUL | *Gephyrocapsa muellerae* | *Emiliania huxleyi* | Medium-sized *Gephyrocapsa* with an oblique bridge |
| 2PLAC | *Pseudoemiliania lacunosa* | *Gephyrocapsa oceanica* | Circular placolith with a large central opening and a distal shield with slits |
| 2PLACWS | *Pseudoemiliania lacunosa* (without slits) | *Gephyrocapsa oceanica* | Circular placolith with a large central opening and a distal shield without slits |
| 2POVA | *Pseudoemiliania ovata* | *Gephyrocapsa oceanica* | Ovoid placolith with a large central opening and a distal shield with slits |
| 2POVAWS | *Pseudoemiliania ovata* (without slits) | *Gephyrocapsa oceanica* | Ovoid placolith with a large central opening and a distal shield without slits |
| 2RHAQ | *Reticulofenestra haqii* | *Gephyrocapsa oceanica* | Medium-sized *Reticulofenestra* with an open central area |
| 2RMIN | *Reticulofenestra minuta* | *Emiliania huxleyi* | Small *Reticulofenestra* with an open central area |
| 2RPROD | *Reticulofenestra producta* | *Reticulofenestra pseudoumbilica* | Medium-sized *Reticulofenestra* with a closed central area |
| 2RPSE | *Reticulofenestra pseudoumbilica* | *Reticulofenestra producta* | Large *Reticulofenestra* |
| | **Coccolithales** | | |
| 3CLEP | *Calcidiscus leptoporus* | *Oolithotus fragilis*, *Calcidiscus mcintyrei* | Circular placolith with a closed or small central area |
| 3CPEL | *Coccolithus pelagicus* | *Coccolithus braarudi* | Large placolith with a bright central area and dark shields |
| 3USI | *Umbellicosphaera sibogae* | | |
| | **Zygodiscales** | | |
| 4HELI | *Helicosphaera carteri* | *Helicosphaera wallishii*, *H. pavimentum* | Helicolith morphology |
| 4PONTO | *Pontosphaera discopora* | *Pontosphaera spp.* | Cribrilith morphology |
| | **Syracosphaerales** | | |
| 4SPUL | *Syracosphaera pulchra* | *Syracosphaera* spp. | Thin elliptical ring with a large central area |
| 7RHABDO | *Rhabdosphaera claviger* | *Rhabdosphaera* spp. | Elongated coccolith resembling a nail |
| 7SCAPH | *Calciosolenia murrayi* | *Calciosolenia* spp. | Lozenge-shaped coccolith (scapholith) |
| | **Incertae sedis** | | |
| 1FLO | *Florisphaera profunda* | | Small, thin polygon coccolith |
| 1GLA | *Gladiolithus flabellatus* | | Small, thin, flat needle-like coccolith with one or two ridges |
| 5UTE | *Umbellosphaera tenuis* | *Umbellosphaera* spp. | Small bright central area surrounded by a large disc with alternating dark and dim radial ornamentation |
| | **Ceratolithaceae** | | |
| 8CERATO | *Ceratolithus cristatus* | *Ceratolithus* spp. | Hook-shaped coccolith |
| | **Discoastrerales** | | |
| 9DISCO | *Discoaster variabilis* | *Discoaster* spp. | Star-shaped coccolith with five or six rays |
| 9SPHENOL | *Sphenolithus abies* (side view) | *Sphenolithus* spp. | Cone-shaped coccolith with spines |
| 9SPHETOP | *Sphenolithus abies* (top view) | *Sphenolithus* spp. | Bulky and small star-shaped coccolith with many rays |

**Table A1. Description of the 28 coccolith classes used to train SYRACOv5. For each class, the class label used by the software, the reference taxon, additional taxa intentionally grouped within the same class because they cannot be reliably distinguished under SYRACO observation conditions, and the main diagnostic morphological features used for manual annotation are indicated. Each class contains 300 manually annotated coccoliths used for model training.**

https://doi.org/10.5194/egusphere-2026-3901
Preprint. Discussion started: 28 July 2026


## Code and data availability

The datasets used to generate the figures (Table S1 – for Fig.4; Table S2 for Fig. 5; Table S3 for Fig. 6 and Table S4 for Fig. 7) presented in this study are available the Supplements.

SYRACOv5 is an operational software platform developed at CEREGE over nearly three decades. It is currently integrated into the MANTA platform, which is under active development to provide web-based access for external users. The source code is available at https://gitlab.osupytheas.fr/manta/v2/analysis. Researchers interested in collaborations or early access are encouraged to contact the corresponding author..

## Supplement link

The link to the supplement will be included by Copernicus, if applicable.

## Author contributions

LB conceived and led the development of SYRACO from its inception and prepared the manuscript with contributions from all co-authors. DD developed the software code for SYRACO versions 1 to 3. YG, NB, MT, AN, and MB contributed to the development of subsequent versions of the software. BSM contributed to the conceptual development of SYRACO since 2014. All authors reviewed and approved the final manuscript.

## Competing interests

A declaration of all potential conflicts of interest is required by Copernicus Publications as this is an integral aspect of a transparent record of scientific work. Please see our competing interests policy.

## Disclaimer

Not applicable.

## Acknowledgements

The authors used an AI-based language assistant during manuscript preparation to improve English style and readability. All scientific content, interpretations and final editorial decisions are the responsibility of the authors.

https://doi.org/10.5194/egusphere-2026-3901
Preprint. Discussion started: 28 July 2026


**Financial support**

This research has been supported by the Agence Nationale de la Recherche (grant no. ANR22 ESDIR 03-ITCH and no. ANR-12-B06-0007-CALHIS), by the Fondation pour la Recherche sur la Biodiversité (FRB-project COCCACE), and by the CNRS-INSU LEFE programme through the SEICEC project.

**Review statement**

The review statement will be added by Copernicus Publications listing the handling editor as well as all contributing referees according to their status anonymous or identified.

**References**

Bach, L. T., Bauke, C., Meier, K. J. S., Riebesell, U., and Schulz, K. G.: Influence of changing carbonate chemistry on morphology and weight of coccoliths formed by Emiliania huxleyi, Biogeosciences, 9, 3449–3463, 10.5194/bg-9-3449-2012, 2012.

Balch, W. M.: The Ecology, Biogeochemistry, and Optical Properties of Coccolithophores, Annual Review of Marine Science, 10, 71–98, https://doi.org/10.1146/annurev-marine-121916-063319, 2018.

Balch, W. M., Bowler, B. C., Drapeau, D. T., Lubelczyk, L. C., and Lyczkowski, E.: Vertical Distributions of Coccolithophores, PIC, POC, Biogenic Silica, and Chlorophyll a Throughout the Global Ocean, Global Biogeochemical Cycles, 32, 2–17, https://doi.org/10.1002/2016GB005614, 2018.

Barbarin, N.: La reconnaissance automatisée des nannofossiles calcaires du cénozoique, Ph.D., Université Aix-Marseille, 245 pp., 2014.

Beaufort, L.: Weight estimates of coccoliths using the optical properties (birefringence) of calcite, Micropaleontology, 51, 289–297, 10.2113/gsmicropal.51.4.289, 2005.

Beaufort, L. and Dollfus, D.: Automatic recognition of coccoliths by dynamical neural networks, Marine Micropaleontology, 51, 57–73, 10.1016/j.marmicro.2003.09.003, 2004a.

Beaufort, L. and Dollfus, D.: Automatic recognition of coccolith by dynamical neural network, Mar. Micropaleont., 51/1-2, 57–73, 2004b.

Beaufort, L. and Grelaud, M.: A 2700-year record of ENSO and PDO variability from the Californian margin based on coccolithophore assemblages and calcification, Progress in Earth and Planetary Science, 4, 10.1186/s40645-017-0123-z, 2017.

Beaufort, L. and Heussner, S.: Seasonal dynamics of calcareous nannoplakton on a west european continental margin: the Bay of Biscay, Marine Micropaleontology, 43, 27–55, 2001.

Beaufort, L., Barbarin, N., and Gally, Y.: Optical measurements to determine the thickness of calcite crystals and the mass of thin carbonate particles such as coccoliths, Nature Protocols, 9, 633–642, 10.1038/nprot.2014.028, 2014.

Beaufort, L., Probert, I., and Buchet, N.: Effects of acidification and primary production on coccolith weight: Implications for carbonate transfer from the surface to the deep ocean, Geochemistry, Geophysics, Geosystems, 8, 10.1029/2006gc001493, 2007.

Beaufort, L., Garidel-Thoron, T. d., Mix, A. C., and Pisias, N. G.: ENSO-like Forcing on Oceanic Primary Production During the Late Pleistocene, Science, 293, 2440–2444, 10.1126/science.293.5539.2440, 2001.

Beaufort, L., van der Kaars, S., Bassinot, F. C., and Moron, V.: Past dynamics of the Australian monsoon: precession, phase and links to the global monsoon concept, Clim. Past., 6, 695–706, 10.5194/cp-6-695-2010, 2010.

Beaufort, L., Couapel, M. J. J., Buchet, N., Claustre, H., and Goyet, C.: Calcite production by Coccolithophores in the South East Pacific Ocean, Biogeosciences 5, 1101–1117, 2008.

https://doi.org/10.5194/egusphere-2026-3901
Preprint. Discussion started: 28 July 2026


Beaufort, L., Gally, Y., Suchéras-Marx, B., Ferrand, P., and Duboisset, J.: A universal method for measuring the thickness of microscopic calcite crystals, based on bidirectional circular polarization, Biogeosciences, 18, 775–785, 10.5194/bg-18-775-2021, 2021.

Beaufort, L., Lancelot, Y., Camberlin, P., Cayre, O., Vincent, E., Bassinot, F., and Labeyrie, L.: Insolation cycles as a major control of the Equatorial Indian Ocean primary production, Science, 278, 1451–1454, 1997.

Beaufort, L., Bolton, C. T., Sarr, A.-C., Suchéras-Marx, B., Rosenthal, Y., Donnadieu, Y., Barbarin, N., Bova, S., Cornuault, P., Gally, Y., Gray, E., Mazur, J.-C., and Tetard, M.: Cyclic evolution of phytoplankton forced by changes in tropical seasonality, Nature, 601, 79–84, 10.1038/s41586-021-04195-7, 2022.

Beaufort, L., Probert, I., Garidel-Thoron, T. d., Bendif, E. M., Ruiz-Pino, D., Metzl, N., Goyet, C., Buchet, N., Coupel, P., Grelaud, M., Rost, B., Rickaby, R. E. M., and Vargas, C. d.: Sensitivity of coccolithophores to carbonate chemistry and ocean acidification, Nature, 476, 80–83, 10.1038/nature10295, 2011.

Berggren, W. A., Kent, D. V., and Couvering, J. A. v.: The Neogene: Part 2 Neogene geochronology and chronostratigraphy, Geol. Soc., Lond., Mem., 10, 211–260, 10.1144/gsl.mem.1985.010.01.18, 1985.

Beuvier, T., Probert, I., Beaufort, L., Suchéras-Marx, B., Chushkin, Y., Zontone, F., and Gibaud, A.: X-ray nanotomography of coccolithophores reveals that coccolith mass and segment number correlate with grid size, Nature Communications, 10, 751, 10.1038/s41467-019-08635-x, 2019.

Bolliet, T., Holbourn, A., Kuhnt, W., Laj, C., Kissel, C., Beaufort, L., Kienast, M., Andersen, N., and Garbe-Schönberg, D.: Mindanao Dome variability over the last 160 kyr: Episodic glacial cooling of the West Pacific Warm Pool, Paleoceanography, 26, 10.1029/2010pa001966, 2011.

Bollmann, J.: Technical Note: Weight approximation of coccoliths using a circular polarizer and interference colour derived retardation estimates – (The CPR Method), Biogeosciences, 11, 1899–1910, 10.5194/bg-11-1899-2014, 2014.

Bollmann, J., Henderiks, J., and Brabec, B.: Global calibration of Gephyrocapsa coccolith abundance in Holocene sediments for paleotemperature assessment, Paleoceanography, 17, 7–1–7–9, 10.1029/2001pa000742, 2002.

Bollmann, J., Quinn, P. S., Vela, M., Brabec, B., Brechner, S., Cortés, M. Y., Hilbrecht, H., Schmidt, D. N., Schiebel, R., and Thierstein, H. R.: Automated particle analysis: Calcareous Microfossils, in: Image Analysis, Sediments and Paleoenvironments, edited by: Francus, P., Kluwer Academic Publishers, Dordrecht, The Netherlands, 2004.

Bory, A., Jeandel, C., Leblond, N., Vangriesheim, A., Khripounoff, A., Beaufort, L., Rabouille, C., Nicolas, E., Tachikawa, K., Etcheber, H., and Buat-Ménard, P.: Downward particle fluxes within different productivity regimes off the Mauritanian upwelling zone (EUMELI program), Deep Sea Res. Part : Oceanogr. Res. Pap., 48, 2251–2282, 10.1016/s0967-0637(01)00010-3, 2001.

Bourel, B., Marchant, R., de Garidel-Thoron, T., Tetard, M., Barboni, D., Gally, Y., and Beaufort, L.: Automated recognition by multiple convolutional neural networks of modern, fossil, intact and damaged pollen grains, Computers & Geosciences, 140, 10.1016/j.cageo.2020.104498, 2020.

Dollfus, D. and Beaufort, L.: Fat neural network for recognition of position-normalised objects, Neural Netw., 12, 553–560, 10.1016/s0893-6080(99)00011-8, 1999.

Duchamp-Alphonse, S., Siani, G., Michel, E., Beaufort, L., Gally, Y., and Jaccard, S. L.: Enhanced ocean-atmosphere carbon partitioning via the carbonate counter pump during the last deglacial, Nature Communications, 9, 2396, 10.1038/s41467-018-04625-7, 2018.

Engel, A., Zondervan, I., Aerts, K., Beaufort, L., Benthien, A., Chou, L., Delille, B., Gattuso, J.-P., Harlay, J., Heemann, C., Hoffmann, L., Jacquet, S., Nejstgaard, J., Pizay, M.-D., Rochelle-Newall, E., Schneider, U., Terbrueggen, A., and Riebesell, U.: Testing the direct effect of CO2 concentration on a bloom of the coccolithophorid Emiliania huxleyi in mesocosm experiments, Limnol. Oceanogr., 50, 493–507, 10.4319/lo.2005.50.2.0493, 2005.

Fuertes, M. A., Flores, J. A., and Sierro, F. J.: The use of circularly polarized light for biometry, identification and estimation of mass of coccoliths, Marine Micropaleontology, 113, 44–55, 10.1016/j.marmicro.2014.08.007, 2014.

Gimenez, B., Joannin, S., Pasquet, J., Beaufort, L., Gally, Y., Garidel-Thoron, T. d., Combourieu-Nebout, N., Bouby, L., Canal, S., Ivorra, S., Limier, B., Terral, J. F., Devaux, C., and Peyron, O.: A user-friendly method to get automated pollen analysis from environmental samples, N. Phytol., 243, 797–810, 10.1111/nph.19857, 2024.

Godbillot, C., Marchant, R., Beaufort, L., Leblanc, K., Gally, Y., Le, T. D. Q., Chevalier, C., and de Garidel-Thoron, T.: A New Method for the Detection of Siliceous Microfossils on Sediment Microscope Slides Using Convolutional Neural

https://doi.org/10.5194/egusphere-2026-3901
Preprint. Discussion started: 28 July 2026


Networks, Journal of Geophysical Research: Biogeosciences, 129, e2024JG008047, https://doi.org/10.1029/2024JG008047, 2024.
Godbillot, C., Pesenti, B., Leblanc, K., Beaufort, L., Chevalier, C., Di Pane, J., Durrieu de Madron, X., and de Garidel-Thoron, T.: Contrasting Trends in Phytoplankton Diversity, Size Structure, and Carbon Burial Efficiency in the Mediterranean Sea Under Shifting Environmental Conditions, Journal of Geophysical Research: Oceans, 130, e2025JC022486, https://doi.org/10.1029/2025JC022486, 2025.
Grelaud, M., Schimmelmann, A., and Beaufort, L.: Coccolithophore response to climate and surface hydrography in Santa Barbara Basin, California, AD 1917-2004, Biogeosciences, 6, 2025–2039, 2009a.
Grelaud, M., Beaufort, L., Cuven, S., and Buchet, N.: Glacial to interglacial primary production and El Niño–Southern Oscillation dynamics inferred from coccolithophores of the Santa Barbara Basin, Paleoceanography, 24, 10.1029/2007pa001578, 2009b.
Guerreiro, C. V., Baumann, K.-H., Brummer, G.-J. A., Fischer, G., Korte, L. F., Merkel, U., Sá, C., Stigter, H. d., and Stuut, J.-B. W.: Coccolithophore fluxes in the open tropical North Atlantic: influence of thermocline depth, Amazon water, and Saharan dust, Biogeosciences, 14, 4577–4599, 10.5194/bg-14-4577-2017, 2017.
He, K., Zhang, X., Ren, S., and Sun, J.: Deep Residual Learning for Image Recognition, 770–778 pp., 10.1109/CVPR.2016.90, 2016.
Henderiks, J.: Coccolithophore size rules - Reconstructing ancient cell geometry and cellular calcite quota from fossil coccoliths, Marine Micropaleontology, 67, 143–154, 10.1016/j.marmicro.2008.01.005, 2008.
Hernández-Almeida, I., Ausín, B., Saavedra-Pellitero, M., Baumann, K. H., and Stoll, H. M.: Quantitative reconstruction of primary productivity in low latitudes during the last glacial maximum and the mid-to-late Holocene from a global Florisphaera profunda calibration dataset, Quaternary Science Reviews, 205, 166–181, https://doi.org/10.1016/j.quascirev.2018.12.016, 2019.
Hopkins, J., Henson, S. A., Painter, S. C., Tyrrell, T., and Poulton, A. J.: Phenological characteristics of global coccolithophore blooms, Global Biogeochemical Cycles, 29, 239–253, https://doi.org/10.1002/2014GB004919, 2015.
Ivanova, E. V., Beaufort, L., Vidal, L., and Kucera, M.: Precession forcing of productivity in the Eastern Equatorial Pacific during the last glacial cycle, Quaternary Science Reviews, 40, 64–77, 10.1016/j.quascirev.2012.02.020, 2012.
Kruijt, A. L., van Dijk, R., Sulpis, O., Beaufort, L., Lassus, G., Brummer, G. J., van der Burg, A. D., Cala, B. A., Ourradi, Y., Peijnenburg, K. T. C. A., Humphreys, M. P., Chaabane, S., Sluijs, A., and Middelburg, J. J.: The contributions of various calcifying plankton to the South Atlantic calcium carbonate stock, Biogeosciences, 23, 531–563, 10.5194/bg-23-531-2026, 2026.
Lassus, G., Beaufort, L., Couapel, M., and Mendels, D.: Taxon-specific coccolithophore carbonate stocks and production across a Pacific trophic gradient from oligotrophic gyre to upwelling zone, EGUsphere, 2026, 1–33, 10.5194/egusphere-2026-3055, 2026.
Le Cun, Y., Boser, B., Denker, J. S., Henderson, D., Howard, R. E., Hubbard, W., and Jackel, L. D.: Backpropagation applied to handwritten zip code recognition, Neural Computation, 1, 541–551, 1990.
Le Mézo, P., Beaufort, L., Bopp, L., Braconnot, P., and Kageyama, M.: From monsoon to marine productivity in the Arabian Sea: insights from glacial and interglacial climates, Clim. Past., 13, 759, 2017.
Marchant, R., Tetard, M., Pratiwi, A., Adebayo, M., and de Garidel-Thoron, T.: Automated analysis of foraminifera fossil records by image classification using a convolutional neural network, J. Micropalaeontol., 39, 183–202, 10.5194/jm-39-183-2020, 2020.
McClelland, H. L. O., Barbarin, N., Beaufort, L., Hermoso, M., Ferretti, P., Greaves, M., and Rickaby, R. E. M.: Calcification response of a key phytoplankton family to millennial-scale environmental change, Scientific Reports, 6, 10.1038/srep34263, 2016.
Meier, K. J. S., Beaufort, L., Heussner, S., and Ziveri, P.: The role of ocean acidification in Emiliania huxleyi coccolith thinning in the Mediterranean Sea, Biogeosciences, 11, 2857–2869, 10.5194/bg-11-2857-2014, 2014.
Milliman, J. D.: Production and accumulation of calcium carbonate in the ocean - budget of a nonsteady state, Global Biogeochem. Cycles, 7, 927–957, 1993.
Morel, A.: An ocean flux study in eutrophic, mesotrophic and oligotrophic situations: the EUMELI program, Deep Sea Res. Part : Oceanogr. Res. Pap., 43, 1185–1190, https://doi.org/10.1016/0967-0637(96)00055-6, 1996.

https://doi.org/10.5194/egusphere-2026-3901
Preprint. Discussion started: 28 July 2026


Muller, M. N., Beaufort, L., Bernard, O., Pedrotti, M. L., Talec, A., and Sciandra, A.: Influence of CO2 and nitrogen limitation on the coccolith volume of Emiliania huxleyi (Haptophyta), Biogeosciences, 9, 4155–4167, 10.5194/bg-9-4155-2012, 2012.

Okada, H. and McIntyre, A.: Seasonal distribution of modern Coccolithophorees in the western north Atlantic ocean, Mar. Biol., 54, 319–328, 1979.

Poulton, A. J., Adey, T. R., Balch, W. M., and Holligan, P. M.: Relating coccolithophore calcification rates to phytoplankton community dynamics: Regional differences and implications for carbon export, Deep Sea Research Part II: Topical Studies in Oceanography, 54, 538–557, https://doi.org/10.1016/j.dsr2.2006.12.003, 2007.

Redmon, J., Divvala, S., Girshick, R., and Farhadi, A.: You Only Look Once: Unified, Real-Time Object Detection, 2016 IEEE Conference on Computer Vision and Pattern Recognition (CVPR), 27–30 June 2016, 779–788, 10.1109/CVPR.2016.91,

Staines-Urías, F., González-Yajimovich, O., and Beaufort, L.: Reconstruction of past climate variability and ENSO-like fluctuations in the southern Gulf of California (Alfonso Basin) since the last glacial maximum, Quaternary Research, 83, 488–501, 10.1016/j.yqres.2015.03.007, 2015.

Su, X., Liu, C. L., and Beaufort, L.: Late Quaternary coccolith weight variations in the northern South China Sea and their environmental controls, Marine Micropaleontology, 154, 10.1016/j.marmicro.2019.101798, 2020.

Su, X., Liu, C., Beaufort, L., Tian, J., and Huang, E.: Late Quaternary coccolith records in the South China Sea and East Asian monsoon dynamics, Glob. Planet. Change, 111, 88–96, 10.1016/j.gloplacha.2013.08.016, 2013.

Suchéras-Marx, B., Giraud, F., Mattioli, E., Gally, Y., Barbarin, N., and Beaufort, L.: Middle Jurassic coccolith fluxes: A novel approach by automated quantification, Marine Micropaleontology 111 15–25, 2014.

Tetard, M., Marchant, R., Cortese, G., Gally, Y., De Garidel-Thoron, T., and Beaufort, L.: Technical note: A new automated radiolarian image acquisition, stacking, processing, segmentation and identification workflow, Clim. Past., 16, 2415–2429, 10.5194/cp-16-2415-2020, 2020.

Valença, C. R., Beaufort, L., Hallegraeff, G. M., and Müller, M. N.: Technical note: A comparison of methods for estimating coccolith mass, Biogeosciences, 21, 1601–1611, 10.5194/bg-21-1601-2024, 2024.

Winter, A., Henderiks, J., Beaufort, L., Rickaby, R. E. M., and Brown, C. W.: Poleward expansion of the coccolithophore Emiliania huxleyi, Journal of Plankton Research, 36, 316–325, 10.1093/plankt/fbt110, 2014.

Young, J. R. and Ziveri, P.: Calculation of coccolith volume and it use in calibration of carbonate flux estimates, Deep Sea Research Part II: Topical Studies in Oceanography, 47, 1679–1700, 10.1016/s0967-0645(00)00003-5, 2000.

Ziveri, P., Langer, G., Chaabane, S., de Vries, J., Gray, W. R., Keul, N., Hatton, I. A., Manno, C., Norris, R., Pallacks, S., Young, J. R., Schiebel, R., Zarkogiannis, S., Anglada-Ortiz, G., Bianco, S., de Garidel-Thoron, T., Grelaud, M., Lucas, A., Probert, I., and Mortyn, P. G.: Calcifying plankton: From biomineralization to global change, Science, 390, eadq8520, doi:10.1126/science.adq8520, 2025.